

Radiation Physics and Engineering 2023; ?(?):?–?

<https://doi.org/>

# Computational study of the effect of sapphire neutron filter on reducing the neutron and secondary-gamma dose rate around the main shield of D channel in TRR

Zohreh Gholamzadeh

Reactor and Nuclear Safety Research School, Nuclear Science and Technology Research Institute (NSTRI), Tehran, Iran

## HIGHLIGHTS

- Sapphire crystal has noticeable impact on the dose rates around a neutron beam line shield.
- Simulation methods are vital to investigate the dose rates behavior without practical high costs.
- Benchmark studies are very important procedures to evaluate the simulation accuracy degree.

## ABSTRACT

Simulation work provides valuable information on the behavior of different research reactor neutron analysis facilities. The present study considered neutron and secondary-gamma dose rate variations by applying a sapphire crystal inside the *D* channel in Tehran Research Reactor (TRR). The MCNPX computational code was used to model the channel and its designed shield. Neutron and gamma dose rates distributions were calculated with a sapphire crystal modeling to investigate the neutron diffraction facility hall dose rates. The data from the dose rate simulations were compared with the experimental data available at a power of 4.2 MW from the research reactor. The comparison showed that there is very good conformity between two data series. The simulated neutron dose rate in front of the main shield overestimated the measurement data by 57% in closed-shutter situation and underestimated the measured data by 32% in open-shutter measurement situation. The investigation has shown that adjusting the crystal size to the channel size is considerably effective, especially at high leakage positions.

## KEYWORDS

Neutron filter  
Neutron and gamma dose rate  
Sapphire crystal  
Tehran Research Reactor  
MCNPX simulation  
Benchmark study

## HISTORY

Received: ?  
Revised: ?  
Accepted: ?  
Published: ?

## 1 Introduction

Newly crystalline materials (mainly single crystals) are effectively used to filter fast neutrons emerging from the neutron beam lines of the research reactors. These crystals decrease noticeably the backgrounds at the sample table of the neutron analysis experiments.

Perfect single crystals can be used as filters to produce a thermal-neutron beam almost free of fast neutron background. The filter material must have a wavelength dependent cross-section in such a way that is low for thermal but strongly increasing at epithermal and high energies. The selection of the filter material and its dimensions are critical parameters affecting the performance of a neutron diffusion instrument (Stamatelatos and Messoloras, 2000).

Several materials such as quartz (SiO<sub>2</sub>), bismuth, silicon, germanium, lead and sapphire (Al<sub>2</sub>O<sub>3</sub>) have been suggested as the most successful neutron filters. Of the

crystals mentioned, only one Al<sub>2</sub>O<sub>3</sub> sapphire crystal was found to be the most efficient fast neutron filter and was incorporated into many neutron instruments (Stamatelatos and Messoloras, 2000). Until now, no database containing thermal cross sections of the most used crystals, such as sapphire is available (Zahar et al., 2016).

The overall cross section  $\sigma_{th}$  is a superposition of several contributions: (a) absorption,  $\sigma_a$ , proportional to neutron wavelength, (b) inelastic,  $\sigma_{inel}$ , and (c) elastic or Bragg scattering,  $\sigma_{ela}$  which depends on neutron wavelength, crystal orientation and crystal perfection. Item (b) depends on crystal temperature (phonon population), where coherent Bragg scattering can be disallowed by using a particular crystal orientation (Zahar et al., 2016):

$$\sigma_{th} = \sigma_a + \sigma_{inel} + \sigma_{ela} \quad (1)$$

The first contribution,  $\sigma_a$ , for sapphire is simply proportional to the neutron wavelength  $\lambda$  and energy in the range

\*Corresponding author: [zgholamzadeh@aeoi.org.ir](mailto:zgholamzadeh@aeoi.org.ir)

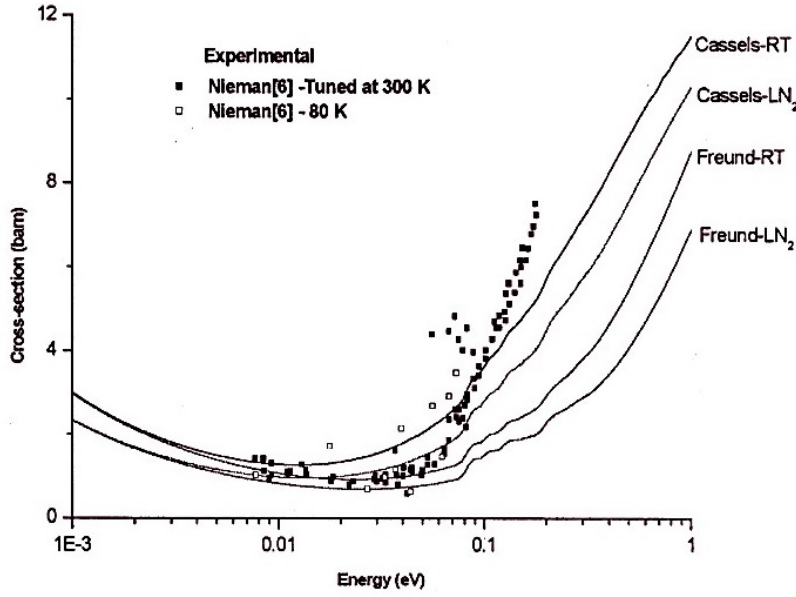


**Figure 1:** Sapphire total neutron cross-section at room and liquid  $N_2$  temperatures (Adib and Kilany, 2003).

( $10^{-4} < E < 10$ ) eV. Thus,  $\sigma_a$  can be written as (Adib and Kilany, 2003):

$$\sigma_a = C_1 E^{-\frac{1}{2}} \quad (2)$$

where  $C_1$  is a constant which can be calculated from values provided by V.F. Sears (Adib and Kilany, 2003).

The second term of Eq. (1) is called thermal diffuse scattering (TLD) or inelastic scattering that is given by (Adib and Kilany, 2003):

$$\sigma_{\text{TLD}} = \left(\frac{A}{1+A}\right)^2 \sigma_{\text{bat}} (1 - e^{-WC_2E}) + E^{-\frac{1}{2}} \begin{cases} (C_1 + \frac{\theta_D^{\frac{1}{2}} \sigma_{\text{bat}}}{36A} R) & \text{for } x \leq 6 \\ (C_1 + \frac{\theta_D^{\frac{1}{2}} \sigma_{\text{bat}}}{36A} 3.3 x^{-\frac{7}{2}}) & \text{for } x > 6 \end{cases} \quad (3)$$

where  $e^{-W}$  is the Debye-Waller factor,  $C_2$  is a constant which is dependent on the scattering material and given by  $C_2 = 4.27 \exp(A/61)$ ,  $X = \theta_D/T$  ( $T$  is the sample temperature),  $\sigma_{\text{bat}}$  is the sum of coherent and incoherent scattering cross-sections of the bound atom),  $A$  in case of compounds is the average atomic mass number, and the series  $R$  is given by

$$R = \sum_{n=0}^{22} \frac{B_n x^{n-1}}{n! (n + \frac{5}{2})} \quad (4)$$

with  $B_n$  that is the Bernoulli numbers.

The optimum filter thickness, the crystal orientation and the temperature give the maximum efficiency of such filter. One can also use the quality factor  $R$ , defined by the ratio of the total cross section at thermal energies,  $\sigma_{\text{th}}$ , to the total cross section at high energies,  $\sigma_{\text{free}}$  (Zahar et al., 2016):

$$R = \frac{\sigma_{\text{th}}}{\sigma_{\text{free}}} \quad (5)$$

In the case of mono-crystalline material, the Bragg scattering cross-section is given by (Adib et al., 2005):

$$\sigma_{\text{Bragg}} = \frac{1}{Nt_0} \ln\left(\frac{1}{T_{\text{Bragg}}}\right) \quad (6)$$

where  $N$  is the number of atoms. $\text{cm}^{-3}$ ,  $t_0$  is the effective thickness of the crystal in cm, and  $T_{\text{Bragg}}$  is the resulting neutron transmission from different  $(hkl)$  planes, given by (Adib et al., 2005):

$$T_{\text{Bragg}} = \prod_{hkl} (1 - P_{hkl}^{\theta}) \quad (7)$$

where  $P_{hkl}^{\theta}$  is the reflecting power of the  $(hkl)$  plane inclined by an angle  $\theta_{hkl}$  to the incident beam direction (Adib et al., 2005). Based on Fig. 1, the researchers measured the total neutron cross section of the sapphire crystal (001).

According to a published manuscript, the absorption cross section of sapphire crystal is 0.231 b at room temperature and its total is 15.7 b (Adib, 2008). Usually other crystals need to cool to present an expected behavior as a good neutron filter. Adib et al. (Adib and Kilany, 2003) showed agreement between calculations and experimental was obtained for values of Bi-single crystals, at room and liquid nitrogen temperatures. Therefore, in the following, a review on the unique sapphire crystal ( $\text{Al}_2\text{O}_3$ ) would be done to reveal its effectiveness for the mentioned purpose.

Adib et al. (Adib et al., 2003) used a simple additive formula that permits the calculation of the nuclear capture, thermal diffuse and Bragg scattering cross-sections as a function of sapphire temperature and crystal parameters. Their results showed that there is an overall agreement between the theoretical formula and experimental data. They suggested the use of sapphire single-crystal as a fast neutron filter in terms of the optimum crystal

thickness, mosaic spread, temperature, cutting plane and tuning for efficient transmission of thermal-reactor neutrons. Their calculation shows that 7.5 cm thick sapphire single crystal, cut along a-axis and with a FWHM on a mosaic spread of 5 min of arc, is a good fast neutron filter. A crystal cut along c-axis with a mosaic spread of about  $1^\circ$  is also an efficient fast neutron filter, when it is fine-tuned to minimize the attenuation for each neutron energy of interest (Adib et al., 2003).

The carried out research by Adib (Adib, 2008) showed a small increase  $\approx 5\%$  at neutron energies  $< 0.02$  eV in the neutron transmission through the cooled sapphire crystal at  $LN_2$  temperatures. Therefore, it can be concluded that the crystal can be used at room temperature with no concerns regarding the reduction of the neutron flux transmitted after the crystal.

Born et al. (Born et al., 1987) have examined the intensity transmitted by a single-crystal of  $Al_2O_3$  over a range of orientation angles within  $\pm 2^\circ$  and did not see any significant change. They have found that a 90 mm-long sapphire-crystal filter has a transmission of about 0.8 for wavelengths in the range (0.12 to 0.24) nm and 0.07 for epithermal neutrons. These transmission results are in good agreement with those obtained by Nieman et al. (Nieman et al., 1980), who suggest that the effective attenuation coefficient can be minimized by fine-tuning of the crystal orientation. Born et al. have found that there is no need to tune the crystals for every wavelength if the crystal mosaic spread is as enough as small. They found that the intensity of the transmitted beam by their crystals does not depend on the orientation of the crystal (Nieman et al., 1980).

Stamatelatos and Messoloras (Stamatelatos and Messoloras, 2000) indicated, the optimum sapphire filter thickness is that which maximizes the slow neutron transmission and minimizes the fast one, so that there is no severe reduction of the thermal neutron flux. Their calculations carried out by these authors showed using 15 cm c-axis sapphire crystal there is 62% transmission of neutrons with 0.11 nm wavelength and 76% transmission for 0.25 nm neutrons. Fast neutron transmission is 3% (Stamatelatos and Messoloras, 2000).

Adib (Adib, 2005) investigated a-axis and c-axis sapphire crystals and indicated that the neutron transmission through 8 cm sapphire single crystal with mosaic spread of

$5'$  along the a-axis is less disturbed by parasitic Bragg reflections than along the c-axis. Since the strong reflections from (119) and (113) planes disturb the neutron transmission along the c-axis  $E \cong 0.02$  eV. As can be also observed parasitic Bragg reflections can limit the use of sapphire as a thermal neutron filter for mosaic spreads  $> 5'$  (Adib, 2005).

Many research reactors have used the sapphire crystal inside their radial neutron beam lines to decrease the neutron/gamma backgrounds at the sample position of their neutron analysis facility (Mishra et al., 2006; Mach, 2018).

In addition, the main shield and sapphire crystal, some shield walls are used around these neutron installations to reduce staff exposures. For example, HANARO Advanced High Flux Neutron Application Reactor is a 30 MW multifunction research reactor located in Dajon, Republic of Korea that uses some zoning shield walls around its neutron diffraction facilities. The shielding walls around the neutron facilities installed in this reactor are made of heavy concrete (<http://www.koreaherald.com/view.php?ud=20140624001075>).

The present work aims to investigate the effect of sapphire crystal on the reduction of neutron and secondary gamma dose rates around the main shield of the Tehran Research Reactor (TRR) diffraction facility.

## 2 Materials and Methods

Tehran research reactor (TRR) is being equipped to a neutron diffraction facility. The reactor core is composed of two types of fuel assembly that are standard fuel elements and control fuel elements. The core consists of 28 standard fuel element (SFE) containing 19-fuel plates and 5 control fuel elements (CFE) containing 14 fuel plates according to the core specifications. The modeled reactor is a 5 MW reactor light water cooled with  $500 \text{ m}^3 \cdot \text{h}^{-1}$  flow rate. Two types of control rods are used in the TRR; which one made out of Ag-In-Cd alloy, and the other of stainless steel. Both have a set of two control plates as a fork type shape. The reactor fuel is  $U_3O_8$ -Al containing 20%-enriched uranium (Mirvakili et al., 2012).

MCNPX code was used to simulate the main shield of TRR diffraction facility (Pelowitz et al., 2005). The simulated main shield details are shown in Fig. 2. The shield has been constructed with the optimized dimensions ac-

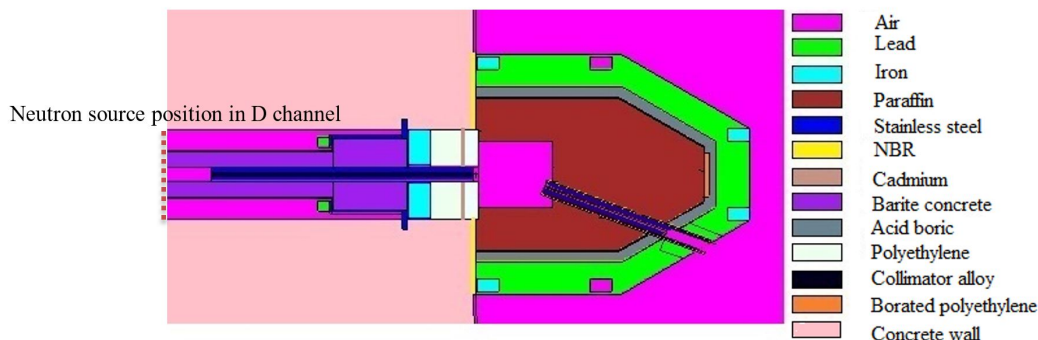


Figure 2: Detail of the used pieces inside  $D$  channel and the main shield simulated using MCNPX.

cording to Ref. (Menarebazari et al., 2022). As in the figure is seen, the shield is composed of three layers; 55 cm paraffin, 5 cm boric acid, 15 cm lead respectively of which the final layer is lead. A monochromator room is seen in the figure with dimension of  $30 \times 40 \text{ cm}^2$  which a 60 cm-long soller collimator installed on its corner would guide the reflected monochromatic neutrons at 20 angel toward outside the shield. After paraffin layer, 1.5 cm thick borated-polyethylene (7%-borated) and 3 mm cadmium sheets of  $20 \times 25 \text{ cm}^2$  were used as thermal neutron beam stop inside the second layer (boric acid).

*D* channel of TRR is a 6-inch radial beam tube that guides the neutrons emerging from the TRR core towards the reactor hall. A high-density concrete collimator holder was used inside the channel according to Fig. 1, the concrete part length is 120 cm. A soller collimator with 120 cm length consist of a stainless steel fram and three narrow sheets which have divided the empty cubic space of the collimatar is used inside the concrete holder. After the concrete holder, an iron disc-shaped piece 10 cm thick is used. Then 15 cm thick polyethylene disc has been used. As a final piece, a borated-polyethylene (7%) of 5 cm thick has been used. A 2 mm cadmium disc was used between the polyethylene disc and the borated-polyethylene disc. Because the main shield would not stand completely fit with the concrete wall of the TRR research reactor, a 2 cm Nitrile Butadin Rubber (NBR) was used between the wall and main shield as flexible neutron shield material.

As the figure shows, different matrials are used to shield the neutron and gamma rays emerged from the *D* channel of TRR. The main shield materials are presented as the following: Air: invironment material, Lead: final gamma shield, Iron: shield first gamma shield inside *D* channel, Paraffin: neutron shield, Stainless steel: soller colimators' material, NBR: flexible neutron shield for the gap between TRR wall and main shield, cadmium: thermal neutron absorber at the designed beam stop window inside acidboric layer, Barite concrete: first soller colimatar holder material, Acid boric: neutron absorber material before lead layer, Polyethylene: heat-resistant neutron moderators inside *D* channel, Collimator alloy: strain-resistant alloy of the soller collimator structure, Borated polyethylen: thermal neutron absorber at the designed beam stop window inside acidboric layer, Concrete wall: the TRR pool wall. The position of the neutron source is shown in the figure with a dash line.

As the figure shows, six iron girders were used at different positions of the main shield structure, which two of them (the middle ones) did not fill with lead during the casting process whereas they were not accessible.

Neutron and gamma sources of TRR were defined in MCNPX input so that their energy spectrum and spatial distribution could give the most precise modeling to the real diffusion of the particles inside the TRR *D* channel (Fig. 3). Then the gamma and neutron dose rates in front of the modeled shield and beside the wall near the NBR layer were calculated. DE/DF card and ANSI/ANS-6.1.1-1977 flux to dose conversion factors were used to calculate the gamma dose rates. Flux to dose conversion factor of NCRP-38, ANSI/ANS-6.1.1-1977 was used to calcu-

late the neutron dose rates. The neutron and gamma dose rates were calculated at different positions around the shield with and without sapphire crystal application inside the *D* channel that is to be installed before the concrete collimator holder. The neutron spectra was defined at the mentioned position according to the Fig. 3 which shows smooth distribution of neutron source without the sapphire crystal, as well as the reduced positional intensity of the neutron source by using the sapphire crystal. Neutron spectra before the sapphire crystal has been shown in Fig. 4.

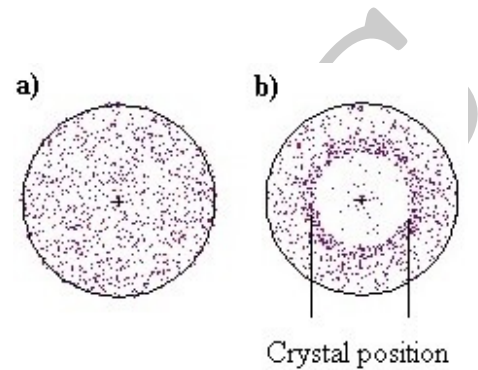


**Figure 3:** Neutron source definition a) smooth distribution without sapphire crystal b) non-smooth distribution with sapphire crystal.

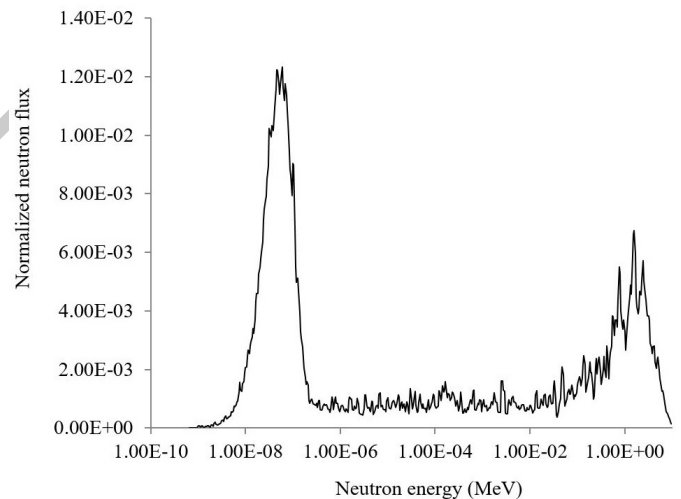


**Figure 4:** Neutron spectra obtained using MCNPX code before first soller collimator holder.

To define the neutron source when a sapphire crystal is used inside the *D* channel, the reduction factor as mentioned by the different experimental and theoretical works was applied for the radial distribution of the neutron source as well as the neutron energy of the spectra. The reduction factor was chosen according to Ref. (Adib, 2008). Hence, the intensity of the neutrons with an energy more than 1 eV was reduced by a 0.9 factor in the spectra shown in Fig. 4. In addition, the radial distribution of

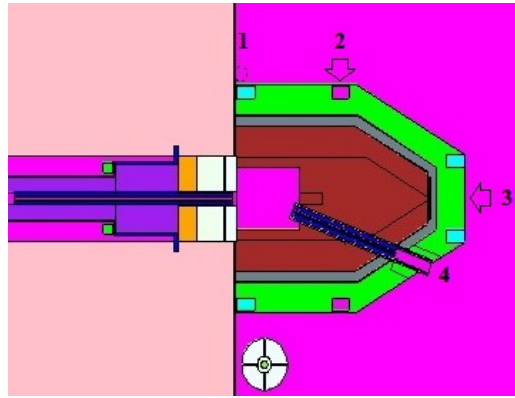


**Figure 5:** The different positions for neutron and gamma dose rates calculations around the main shield of TRR, dxt sphere is observed at position No. 1.

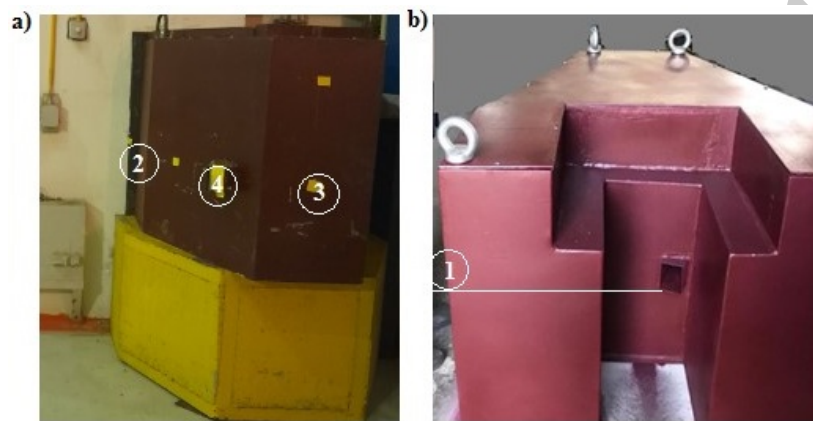


**Figure 6:** The constructed and installed main shield a) front view, b) back view that the second collimator entrance is clear in this view where the point No. 1 and other ones have been selected co-level with it.

neutron spectra was reduced by the same factor, which indicates the crystal position. It should be mentioned any cross section for crystalline materials are not available in the used version of MCNPX code. Therefore, the crystal effects on neutron spectra has been applied for the following simulations and the crystal material was not modeled inside the  $D$  channel. The neutron source was defined by SDEF card before the first soller collimator holder. In addition, the crystal size effect on the neutron and gamma dose rates was investigated using enhancement of the crystal diameter in the neutron source definition of the MCNPX SDEF card. Clearly, reduction of the neutrons using the sapphire crystal would decrease the secondary gamma dose rates. Therefore, neutron dose rate and secondary gamma dose rate tallies were used in the MCNPX code input file for any code being performed. Mesh tally card was applied to determine the neutron and gamma dose rate distributions around the modeled shield. In addition, the primary gamma dose rates were calculated using a smooth gamma source definition in the MCNPX code input. Figure 5 shows the positions (No. 1 up to No. 4) that the neutron and gamma dose rates were calculated around the main shield of the TRR  $D$  channel. A shutter also is being designed for the shield to avoid any neutron and gamma departure from the second soller collimator

towards the TRR hall when the facility is not under operation. In the present work, the gamma and neutron dose rates of the position No. 3 were calculated in open shutter situation.

Figure 6 shows the constructed and installed main shield which has been modeled in detail by MCNPX code.

Dextran card (dxt) was used for the calculations as a variance reduction method to decrease the statistical errors of the calculations. Neutron flux distribution of thermal energy range ( $E_n < 0.4$  eV) and fast energy range ( $E_n > 1$  keV) were calculated using mesh tally card of the used computational code too.

Finally, a benchmark study was carried out for position No. 3 at 4.2 MW operation of TRR to verify the obtained simulation data accuracy.

### 3 Results and Discussion

Neutron and gamma dose rates were calculated for position No. 1 (beside the concrete wall gap), position No. 2 (in front of the empty iron girder), position No. 3 (in front of the main shield third layer in direct beam leakage path) and position No. 4 (in front of the second soller collimator exit). The obtained results presented in Table 1 show that in the case of position No. 1, the neutron dose rate

**Table 1:** Neutron dose rate of different positions around the *D* channel main shield.

Position number	No. 1 ( $\mu\text{Sv.h}^{-1}$ )	No. 2 ( $\mu\text{Sv.h}^{-1}$ )	No. 3 ( $\mu\text{Sv.h}^{-1}$ )	No. 4 ( $\mu\text{Sv.h}^{-1}$ )
Without sapphire	8930	6520	314	580
With sapphire Dia. 14 cm	2580	966	155	270
With sapphire Dia. 15 cm	1256	853	153	264

**Table 2:** Secondary gamma dose rate of different positions around the *D* channel main shield.

Position number	No. 1 ( $\mu\text{Sv.h}^{-1}$ )	No. 2 ( $\mu\text{Sv.h}^{-1}$ )	No. 3 ( $\mu\text{Sv.h}^{-1}$ )	No. 4 ( $\mu\text{Sv.h}^{-1}$ )
Without sapphire	3160	1000	5.4	222
With sapphire Dia. 14 cm	1170	395	4.2	12.3
With sapphire Dia. 15 cm	1162	314	4.1	10.2

could be reduced from about  $9 \text{ mSv.h}^{-1}$  to  $1 \text{ mSv.h}^{-1}$  by using sapphire crystal, which the drop is noticeably. It should be mentioned that the *D* channel diameter is about 16 cm. The calculations showed that in this position, by changing the crystal diameter from 14 cm to 15 cm, the neutron dose rate would be reduced by half ( $2.580 \text{ mSv.h}^{-1}$  to  $1.256 \text{ mSv.h}^{-1}$ ). The obtained results for position No. 2 showed that using the sapphire crystal would result in a high reduction of the neutron dose rate at this position but (about 6.5 times). However, the crystal size enhancement would not have a noticeable effect on the neutron dose rate reduction at this position (only about 11.6%). In the case of position No. 3, application of sapphire crystal inside the *D* channel would reduce the neutron dose rate by half. The low reduction of the neutron dose rate at this position is resulted as the fact that the crystal is fast neutron shield so the most arrived neutrons to this position are thermal hence thermal flux had not much reduction in direct neutron beam path with and without sapphire crystal. In addition, the crystal size enhancement would not have any effect on the neutron dose rate at position No. 3 ( $155 \pm 7.9 \mu\text{Sv.h}^{-1}$  to  $153 \pm 8.7 \mu\text{Sv.h}^{-1}$ ) so it can be said the difference between the values is in the statistical error range of about 5%. The carried out calculations showed that according to Table 1, the neutron dose rate would be reduced by half at position No. 4 ( $580 \mu\text{Sv.h}^{-1}$  to  $270 \mu\text{Sv.h}^{-1}$ ) using a sapphire crystal at *D* channel of TRR. In addition, the crystal size reduction has not any noticeable effect on neutron dose rate reduction at this position. The same reasons for position No. 3 could be accounted for position No. 4, while the second collimator body is stainless steel (a fast neutron scattering material). In overall, the calculations indicate that the crystal has a high effect on the neutron dose rate for the positions that have high neutron leakage without experiencing many moderator materials.

Clearly, it would be expected that the secondary gamma dose rates are reduced by using sapphire crystal inside the *D* channel of TRR. Table 2 shows the obtained results of the secondary gamma dose rate calculations. According to Table 2, position No. 1 gamma dose rate would be reduced to one third using sapphire crystal. Position No. 2 shows the same behavior. Position No. 3 gamma dose rate would be reduced slightly (about 22%) by using sapphire crystal as the fact that the highest ( $n, \gamma$ ) reac-

tion rates inside paraffin belong to low energy neutrons which are not filtered by the crystal. Application of the sapphire crystal has a noticeable effect on the gamma dose rate of position No. 4, which is the second collimator exit position. In the case of all the positions, the crystal size enhancement has no obvious effect on the gamma dose rate reduction.

In overall, it can be said the most affected positions of the crystal size are No. 1 owing to its high neutron leakage and No. 4 owing to its high gamma leakage.

Mesh tally was used to map the dose rates around the main shield. The calculations were carried out with the expectation of a 15 cm-diameter sapphire crystal presence inside the *D* channel. The carried out calculations showed that the average neutron dose rate in front of the main shield is about  $100 \mu\text{Sv.h}^{-1}$  while the values increase near the concrete wall where the highest neutron leakages are possible. The mesh tally calculations showed that in front of the main shield the average gamma dose rate is about  $116 \mu\text{Sv.h}^{-1}$  (Fig. 7).

Neutron flux distribution around the main shield was investigated using mesh tally according to Fig. 8. As the figure shows near the concrete wall, the average total neutron flux changes from  $10^4 \text{ n.s}^{-1}.\text{cm}^{-2}$  up to  $10^5 \text{ n.s}^{-1}.\text{cm}^{-2}$  while in front of the main shield the value decreases to the order of  $10^3 \text{ n.s}^{-1}.\text{cm}^{-2}$ . In addition, the figure shows the fast neutron flux in front of the main shield would be in order of less than  $34 \text{ n.s}^{-1}.\text{cm}^{-2}$ .

Figure 9 shows the primary gamma distribution around the main shield. The carried out investigations showed the average gamma dose rate is about  $18 \mu\text{Sv.h}^{-1}$  in front of the main shield while the highest leakage is observed around the empty girders.

The carried out investigations show there needs to be reinforced near the empty iron girders as well as the gap between the concrete wall and the main shield, especially in view of neutron shielding. It should be mentioned construction of a bigger main shield was not possible on account of its weight limitations. In addition, the facility is to be used for diffraction equipment, where the bigger shield would disturb proper installation of the equipment. Hence, the local reinforcements would damp the high exposure problems around the main shield.

Neutron and gamma dosimetry was carried out at position No. 3, which has been depicted in Fig. 5, which is a

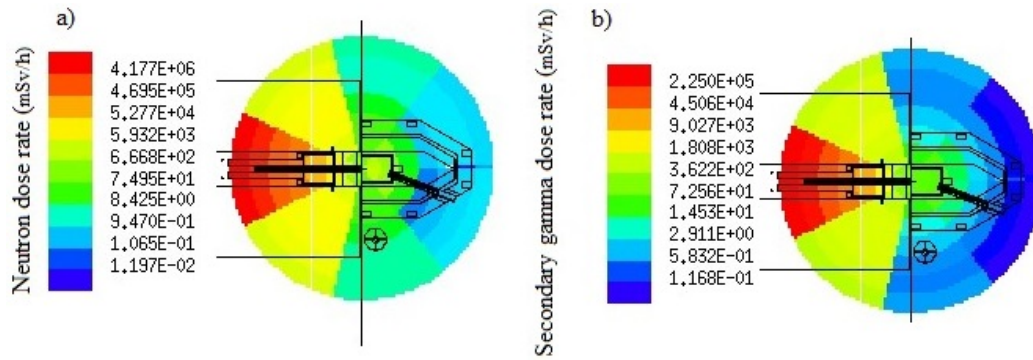


Figure 7: Dose rate distribution around the main shield of the TRR *D* channel a) Neutron b) Secondary gamma.

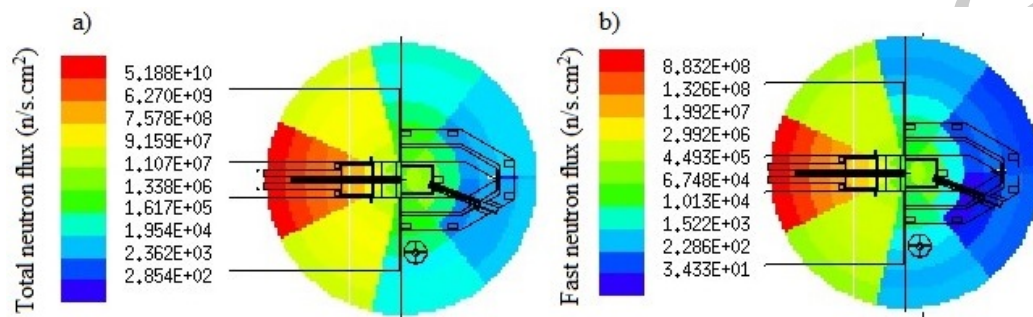


Figure 8: Neutron flux distribution around the main shield of the TRR *D* channel a) Total b) Fast.

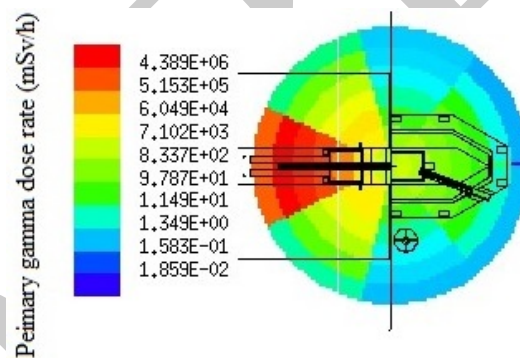


Figure 9: Primary gamma dose rate distribution around the main shield of the TRR *D* channel.

location exactly in the middle of the direct beam leakage after the lead layer of the main shield. The measurement was done at different TRR powers (Fig. 10). According to the figure, the simulated neutron dose rate is 1.57 times (57%) higher than the measured value at 4.2 MW power in the situation of a closed unfit shutter installed on the second soller collimator exit. The simulation value was 32% less than the measured neutron dose rate at 4.2 MW in open shutter situation of the second soller collimator.

The carried out benchmark study showed good agreement between the simulation and experimental data. The observed discrepancy between the two data is arisen from the fact the dose rate calculations could not be done using KCODE mode of the MCNPX code which involves completely the research core geometry with the installed facility on its *D* channel. Complication of the modelled

geometry would result in long run times of the computational code, mainly several months. Moreover, the final run statistical errors would not be acceptable. So, the neutron and gamma sources were calculated using KCODE mode at the entrance of the first soller collimator, then the sources were defined in another MCNPX input involving only *D* channel beam line and its shield, not the whole TRR core. Hence, this discretization would result in some calculation errors itself. The facility beam shutter has not been completed yet. The above-mentioned measurement plots have been done using another unfit shutter, so the in front dose rate measured values may be less when a fit shutter is installed. The TRR core configuration is another reason for the observed discrepancies between simulation and experimental data. It should be mentioned the TRR core configuration might change in every oper-

ation run, which would result in variation of the source terms even up to 30%. The used dosimeter uncertainties in experimental measurements would be another reason for the observed discrepancies between the simulation and experimental data.

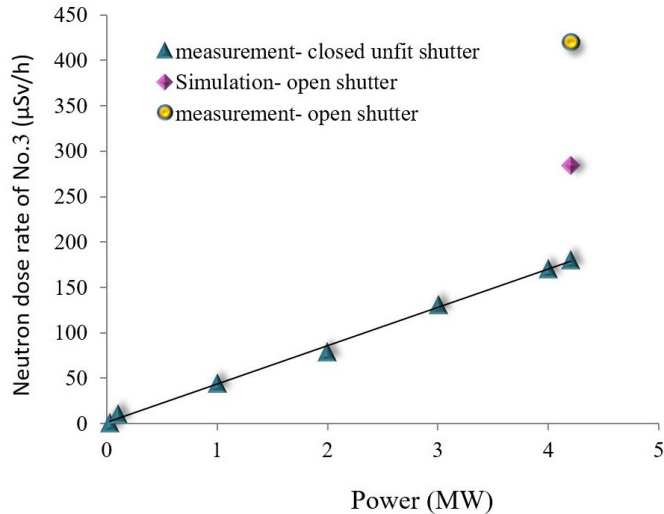


**Figure 10:** Comparison of neutron dose rate measurement and simulation at position No. 3 (in front of the main shield) .

## 4 Conclusion

Simulation data before installation of the neutron facilities in the research reactors could effectively guide the researches and the beam line operators to design the suitable required shield material around the facility. The present work using MCNPX code to simulate TRR  $D$  channel is to be applied to monochromatic neutron cross section measurement with different materials. The carried out simulation showed that the sapphire crystal application inside the beam channel would drastically decrease the neutron dose rates around the main shield of the  $D$  channel especially in high-leaked neutron positions. Fitting the sapphire crystal with the  $D$  channel diameter would not have a significant effect on the experienced neutron dose rate of the different investigated positions except the position No. 1 where the dose rate reduction is about half because of the excessive leakage of the neutrons from this position (gap between the concrete wall and the main shield). Whereas the neutron flux reduction by using the sapphire crystal inside the  $D$  channel would result in secondary gamma reduction, the secondary gamma dose rates were calculated. The calculations showed that the crystal application reduces the secondary gamma dose rate noticeably (about 3 times) at positions No. 1 and No. 2 which are the high-leaked gamma positions. The crystal size fitting with the  $D$  channel diameter has no significant effect on the secondary gamma dose rates (because the variation is in the range of statistical calculation errors of  $\sim 5\%$ ), except position No. 2 which is a high-leaked gamma area. The crystal diameter enhancement from 14 cm to 15 cm would result in 20% reduction of the secondary gamma dose rate at position No. 2. In overall, the calculations

indicate the high-leaked positions need reinforcement and the sapphire crystal size should be as possible as fit with the  $D$  channel size without considerable gap when it is installed inside the channel. The study also helped to select the proper partitioning that was to be done around the facility to protect the reactor personnel from high radiation exposures.

## References

- Adib, M. (2005). Cross-section of single-crystal materials used as thermal neutron filters.
- Adib, M. (2008). Attenuation of Reactor Gamma Radiation and Fast Neutrons Through Large Single-Crystal Materials. *Proceedings of the 3<sup>rd</sup> Environmental Physics Conference*, 19-23 Feb. 2008, Aswan, Egypt, pp.257-272.
- Adib, M. and Kilany, M. (2003). On the use of bismuth as a neutron filter. *Radiation Physics and Chemistry*, 66(2):81–88.
- Adib, M., Kilany, M., Habib, N., et al. (2003). Neutron Transmission of Single-Crystal Sapphire Filters. *4<sup>th</sup> Conference on Nuclear and Particle Physic; EG0600145*, 11-15 Oct. 2003, Fayoumi, Egypt, pp.224-237.
- Adib, M., Kilany, M., Habib, N., et al. (2005). Neutron transmission of single-crystal sapphire filters. *Czechoslovak Journal of Physics*, 55(5):563–578.
- Born, R., Hohlwein, D., Schneider, J., et al. (1987). Characterization of a sapphire single crystal for the use as filter in thermal neutron scattering. *Nuclear Instruments and Methods in Physics Research Section A: Accelerators, Spectrometers, Detectors and Associated Equipment*, 262(2-3):359–365.
- Mach, W. (2018). *Installation of a neutron beam instrument at the TRIGA reactor in Vienna*. PhD thesis, Wien.
- Menarebazari, Z. A., Jafari, H., Gholamzadeh, Z., et al. (2022). The design and optimization of a radiation shield for the Tehran Research Reactor's neutron diffraction facility. *Progress in Nuclear Energy*, 148:104224.
- Mirvakili, S., Keyvani, M., Arshi, S. S., et al. (2012). Possibility evaluation of eliminating the saturated control fuel element from Tehran research reactor core. *Nuclear Engineering and Design*, 248:197–205.
- Mishra, K. K., Hawari, A. I., and Gillette, V. H. (2006). Design and performance of a thermal neutron imaging facility at the North Carolina State University PULSTAR reactor. *IEEE Transactions on Nuclear Science*, 53(6):3904–3911.
- Nieman, H., Tennant, D., and Dolling, G. (1980). Single crystal filters for neutron spectrometry. *Review of Scientific Instruments*, 51(10):1299–1303.
- Pelowitz, D. B. et al. (2005). MCNPX users manual. *Los Alamos National Laboratory, Los Alamos*, 5:369.
- Stamatelatos, I. and Messoloras, S. (2000). Sapphire filter thickness optimization in neutron scattering instruments. *Review of Scientific Instruments*, 71(1):70–73.
- Zahar, N., Benchekroun, D., Belhorma, B., et al. (2016). Study of Sapphire and MgO as Thermal Neutron Filters for The TRIGA Moroccan Reactor Beam ports. *International Journal of Advanced Research*, 4(7):560–567.